then the transport equations. In principle, this option looks promising, but it requires powerful computers, sophisticated software programs, and a large amount of computing time. The other approach consists in elaborating a relatively simple analytical model that would phenomenologically take account of anomalous losses and allow a simple and rapid solution. In all likelihood, theorists will work along both lines.

III. Search for limiting density in stellarators. The fact that limiting density has not thus far been found in stellarators does not mean that it is altogether nonexistent. The solution to this problem is of primary importance because it would permit achieving the ignition conditions of a fusion reaction at lower temperatures.

IV. Diverter performance testing. A reactor cannot work without a diverter. However, an optimal design of a diverter remains to be developed and its efficiency needs to be assessed more thoroughly.

V. Extension of international collaboration, creation of comprehensive experimental database, and specification of scaling properties. Cooperation between different research groups in the framework of the stellarator program has been successfully developing in the past years in the form of exchange of scientists, the organization of joint working groups for the collection and analysis of experimental data obtained at different facilities, regular meetings to discuss newly obtained results, joint exploitation of powerful computers, and extensive use of Internet resources.

VI. Improvement of plasma parameters to be achieved by using more powerful facilities and enhancing power of plasma heating sources.

VII. Elaboration of a stellarator-based reactor project. Although building a stellarator-based fusion reactor is not a matter for tomorrow, the work toward this goal needs to be carried out today because many problems apart from purely physical ones (engineering, technological, economic, etc.) will have to be resolved. The development and construction of ITER would be of great help in this context.

I cannot help observing here that unfortunately the presence of Russian scientists in international efforts within the framework of the world stellarator program is rapidly decreasing. The same is true of the tokamak program and collaboration between Russian and foreign researchers. The causes are well known: from the lack of adequate financial support (and, as a consequence, the absence of new experimental devices and modern diagnostic equipment) to the aging of research groups, loss of interest, and unwillingness of young specialists to associate themselves with science, plus the waning prestige of the scientist at large. With this in mind, it appears safe to predict that the participation of Russia in the ITER program may end in complete failure for the simple reason that there will be nobody to recruit into it.

To conclude, I would like to say a few words about the man whose memory has brought us all together here.

I was not an intimate friend of Boris Borisovich Kadomtsev nor even his close associate, but I frequently met with him at numerous conferences, seminars, and workshops. What always impressed me was his remarkable physical intuition. Within a few days after a new experimental effect or phenomenon was reported, Boris Borisovich explained its physical nature in hand-waving terms speaking at a seminar or in a narrow circle of colleagues. Surprisingly, this first explanation of his was exactly in line with what was postulated after a time by a well-considered theory or in his own work. Surely, B B Kadomtsev was an outstanding scientist, a heaven-sent theorist. His death is an irreparable loss, not only for the plasma community but also for physics in general. He will be sorely missed by all who knew him. The sole consolation is the splendid reviews and those (alas!) few monographs [10–13] that he left to be studied, as I hope, by seasoned researchers and fledgling students alike.

References

1. Galeev A A, Sagdeev R Z *Zh. Eksp. Teor. Fiz.* **53** 359 (1967) [*Sov. Phys. JETP* **26** 1115 (1968)]
2. Kovrizhnykh L M *Zh. Eksp. Teor. Fiz.* **56** 877 (1969) [*Sov. Phys. JETP* **29** 475 (1969)]
3. Kovrizhnykh L M "Protsessy perenosa v toroidal'nykh lovushkakh stellaratornogo tipa" ("Transport processes in stellarator type magnetic traps"), Preprint No. 222 (Moscow: FIAN, 1982); *Nucl. Fusion* **24** 851 (1984)
4. Kovrizhnykh L M *Zh. Tekh. Fiz.* **31** 888 (1961); **32** 526 (1962) [*Sov. Phys. Tech. Phys.* **6** 643 (1962); **7** 316 (1962)]
5. Morozov A I, Solov'ev L S, in *Voprosy Teorii Plazmy* (Topics in Plasma Theory) Issue 2 (Ed. M A Leontovich) (Moscow: Gosatomizdat, 1963) p. 3
6. Kovrizhnykh L M, Shchepetov S V *Fiz. Plazmy* **6** 976 (1980) [*Sov. J. Plasma Phys.* **6** 533 (1980)]
7. Strauss H R *Plasma Phys.* **22** 733 (1980)
8. Kovrizhnykh L M, Shchepetov S V *Pis'ma Zh. Eksp. Teor. Fiz.* **33** 441 (1981) [*JETP Lett.* **33** 425 (1981)]
9. Popov S N, Popryadukhin A P *Zh. Tekh. Fiz.* **36** (2) 390 (1966) [*Sov. Phys. Tech. Phys.* **11** 284 (1967)]
10. Kadomtsev B B *Kollektivnye Yavleniya v Plazme* (Collective Phenomena in Plasma) 2nd ed. (Moscow: Nauka, 1988) [Translated into English in *Reviews of Plasma Physics* Vol. 22 (Ed. V D Shafranov) (New York: Kluwer Acad./Plenum Publ., 2001) p. 1]
11. Kadomtsev B B *Tokamak Plasma: A Complex Physical System* (Bristol: IOP Publ., 1992)
12. Kadomtsev B B *Dinamika i Informatsiya* (Dynamics and Information) 2nd ed. (Moscow: Redaktsiya Zhurnala "Uspekhi Fizicheskikh Nauk", 2001)
13. Kadomtsev B B *Na Pul'sare* (On the Pulsar) (Izhevsk: RKhD; Moscow: Redaktsiya Zhurnala "Uspekhi Fizicheskikh Nauk", 2001) [Translated into English (London: World Scientific, 2009) (in press)]

PACS numbers: **52.80.–s**, 92.60.Pw, 94.20.wq
DOI: 10.3367/UFNe.0179.200907h.0779

Nonlinear phenomena in the ionospheric plasma. Effects of cosmic rays and runaway breakdown on thunderstorm discharges

A V Gurevich, A N Karashtin, V A Ryabov, A P Chubenko, A L Shepetov

1. Introduction

This article reviews some recent progress in the theory of cosmic rays and runaway breakdown (RB) along with new observations of their effects on thunderstorm processes in the atmosphere. An asymptotic solution of the linear kinetic equation is considered and similarity relations for runaway breakdown are proposed. The paper describes the Groza experimental installation measuring different forms of radiation during thunderstorms that is operated at the high-altitude cosmic ray station of the P N Lebedev Physical

Institute, RAS, located in the mountains of Tien Shan. The main concern is with observations of intense gamma-ray bursts in the active phase of thunderstorms. Specific atmospheric discharges caused by the joint action of runaway breakdown and extensive air showers on a thundercloud are recorded for the first time. The discovery of intense long-lasting gamma bursts and their correlation with radio emission gives the first experimental evidence of the key role of cosmic ray-initiated runaway breakdown in charge accumulation and transfer from clouds to a lightning leader during an active thunderstorm period.

The thunderstorm discharge, i.e., the lightning, is a result of three major processes:

(1) Accumulation of electric charges from a large mass of clouds (in fact, the initiation of lightning) in which they are resided on water droplets or small pieces of ice.

(2) Charge transfer from the cloud to the ground or between clouds.

(3) 'Burning' of the charge in the thunderstorm discharge (lightning proper).

The third process — return stroke of lightning — is fairly well known and has been studied rather extensively. The second one (formation of the lightning leader) is studied equally well, although many its aspects await further clarification. The first one has not been discussed in the literature at any length.

The fact is that earlier investigators observed radio emission from multiple discharges proceeding in the cloud. These discharges were believed to result from conventional air breakdown. However, numerous measurements (very accurate of late) have shown that the electric field in thunderclouds never reaches the strength necessary to initiate a normal atmospheric discharge (as definitively confirmed by recent explorations [1, 2]). For this reason, charge accumulation from a large mass of clouds remains an open issue, virtually untouched in the literature (see, e.g., monographs [3, 4]).

The present report demonstrates for the first time that the active phase of a thunderstorm discharge is actually accompanied by powerful gamma-ray fluxes in the clouds and radio emission correlated with gamma radiation. It suggests runaway breakdown. The electric field is stronger than the critical field characteristic of runaway breakdown. The breakdown is triggered by secondary electrons of cosmic rays (CRs). Therefore, the runaway breakdown in the clouds may account for charge accumulation from clouds, necessary for a thunderstorm discharge to be produced. This opens up a new line of inquiry for the study of the first and main phase — the basic process of thunderstorm discharge. The whole problem is closely related to the ideas and concepts of plasma physics developed in the principal works of B B Kadomtsev. To recall, runaway breakdown is a process in which any matter behaves like a plasma.

Atmospheric discharges have been extensively investigated in recent years. New forms of discharges between atmosphere and ionosphere (sprites, elves, and blue jets) have been discovered [5, 6]. Strong terrestrial gamma flashes (TGFs) have been recorded [7]. High-altitude discharges generating superpowerful radio pulses, i.e., narrow bipolar events (NBEs), have been thoroughly studied [8].

The results of new measurements have posed new questions. By way of example, the latest work has given indisputable experimental evidence that the electric field strength E in the clouds is much lower than the threshold

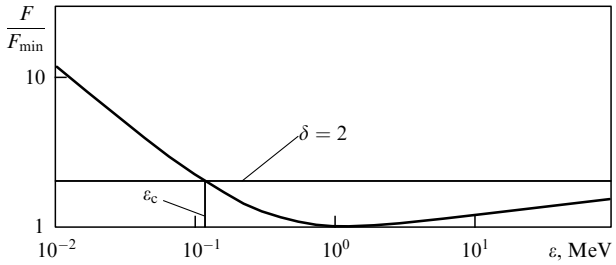

Figure 1. Dependence of braking force F on electron energy ε. Force F is normalized to $F_{\min}$, and the parameter $\delta = E/E_c$.

electric breakdown E_{th} [1, 2, 9]. How then is lightning initiated? How do numerous discharges generating radio emission bursts develop in the active period of a thunderstorm [10]? The new physical process, *runaway breakdown*, helps to answer these questions [11, 12]. RB has a low excitation threshold corresponding to electric fields present in the thunderstorm atmosphere.

Conventional breakdown results from the heating of electrons in an electric field. In this process, fast electrons that belong to the tail of the distribution function become able to ionize matter and, therefore, to generate new free electrons, while slow electrons disappear either owing to recombination in the bulk or on the walls of the discharge chamber. As soon as the electric field becomes sufficiently strong, the generation of new electrons via ionization exceeds their disappearance due to recombination, and their number begins to increase exponentially. This phenomenon is termed electric breakdown of matter. Characteristic energies of electrons responsible for ionization are 10–20 eV, while recombination mostly takes place at low energies. For this reason, mean electron energy $\bar{\varepsilon}$ does not normally exceed several electron-volts. For instance, this energy in the air is $\bar{\varepsilon} \sim 2$ eV.

Runaway breakdown has an essentially different nature [13], resulting from the interaction between fast particles and matter. The braking force F acting on an energetic particle in matter is determined by ionization losses [14]. Figure 1 shows that force F decreases with increasing electron energy $\bar{\varepsilon}$ because fast electrons interact with the electrons and nuclei of neutral matter as if they were free particles, i.e., according to the Coulomb law. The Coulomb scattering cross section is the Rutherford cross section $\sigma \sim 1/\varepsilon^2$. That is why the braking force $F \sim \varepsilon\sigma N_m \sim 1/\varepsilon$ in the nonrelativistic region where it is proportional to molecular number density N_m and inversely proportional to the electron energy ε. The decrease in the ionization braking force becomes weaker due to relativistic effects. For $\varepsilon \geqslant 1$ MeV, it falls to a minimum and thereafter begins to slowly (logarithmically) increase (see Fig. 1).

The decrease in the friction force is related to the possibility of the appearance of runaway electrons in a substance placed in an electric field. Indeed, if a constant field E is present in a medium, such that $E > E_c = F_{\min}/e$, an electron with a sufficiently high energy $\varepsilon > \varepsilon_c$ will be continuously accelerated by the field (see Fig. 1). Such electrons are called runaway electrons [15].

Runaway breakdown is associated with the generation of secondary electrons due to the ionization of neutral molecules by fast runaway particles. Although the majority of secondary electrons have low energies, electrons with rather high energy $\varepsilon > \varepsilon_c$ can be produced as well. These will also become runaway electrons, i.e., they will be accelerated by the field

(see Fig. 1), and may in turn generate particles with $\varepsilon > \varepsilon_c$ in the ionization process. As a result, an exponentially growing avalanche of runaway electrons develops. In parallel, an immensely large number of slow electrons are generated, which ultimately leads to an electric breakdown of the matter. It is of importance that runaway breakdown occurs in a relatively weak field $E \geqslant 1.3E_c$ which is an order of magnitude smaller than the field strength E_{th} of conventional electric breakdown. For instance, $E_{th} \approx 23$ kV cm^{-1} and $E_c \approx 2.16$ kV cm^{-1} at atmospheric pressure in the air.

However, condition $E \geqslant 1.3E_c$ alone is insufficient for runaway breakdown to develop. The presence of fast bare electrons with energies in excess of critical runaway energy $\varepsilon > \varepsilon_c$ is necessary. Such electrons effectively generated by cosmic rays are always present in the atmosphere. They are responsible for RB during thunderstorms and its action on the development of atmosphere electric discharges in the active thunderstorm period.

This period comprises several stages, namely, preliminary breakdown, the formation and motion of leaders, the main return stroke, repetitive return strokes, etc. It may be supposed that in the active period the in-cloud electric field exceeds E_c in a broad zone [1] and can be even higher, $E > E_{th}$, in local areas (e.g., in the leader core) [3]. In these areas, RBs may locally develop, accompanied by gamma-ray and radio pulses. The existence proof of RB and revealing of its participation in atmosphere discharges would be direct observation of high-energy electrons and gamma-ray pulses inside thunderstorm clouds, since neither travels a long distance. It should be noted that an important role is played not only by secondary electrons with energies ranging $10^4 - 10^6$ eV but also by primary CR particles with energies of $10^{14} - 10^{16}$ eV initiating extensive air showers (EASs). 'Cloud-to-ground' lightning is typically generated at an altitude of 4–6 km, corresponding to the characteristic altitude of the maximum number of particles in the showers produced by CR with an energy in excess of 10^{15} eV. Hence the extreme importance of the facility operating at such altitudes for comprehensively surveying high-energy CRs, gamma-ray, X-ray, and radio emissions from lightning discharges.

The Tien Shan high-altitude cosmic ray station of P N Lebedev Physical Institute (TSCRS) is a unique site for investigations into the physics of thunderstorm discharges. Its Groza installation is designed to systematically study atmospheric discharges and simultaneously record different types of radiation (electron, gamma, X-ray, and radiofrequency) in the range from 0.1 to 30 MHz and at a frequency of 250 MHz. It has been collecting statistics for several years now. All its detectors continuously operate in the automatic mode during the thunderstorm season (May–September). An important advantage of this installation is its location at an altitude between 3340 and 4000 m above sea level, where thunderstorm clouds are formed in the mountains of northern Tien Shan; in other words, its detectors are sort of embedded in the clouds.

The very first data suggesting markedly enhanced radiation in a range of 100–500 keV during thunderstorms were obtained as early as 2002 [16]. Thereafter, correlation between short radio pulses and the arrival of EASs was documented [17]. Bipolar pulses of short-wave (SW) radio emission coincident (within 50 μs) with trigger signals of the EAS recording system were observed. Such pulses never occurred in the absence of a thunderstorm. Later investigations showed that SW radio emission from each stroke of lightning starts as a short bipolar pulse with a rise time of order 100 ns [20], similar to what was observed in lowland terrains [18, 19]. The shape, width, and amplitude of the initial pulse were consistent with the respective values predicted by the theory of joint RB/EAS action induced by a primary particle with an energy of $10^{15} - 10^{16}$ eV.

This paper presents results of new observations of the influence of CRs and RB on thunderstorm processes in the atmosphere. Section 2 contains brief remarks on the theory of RB. In Section 3, we describe the Groza experimental installation measuring different types of radiation during thunderstorms. Section 4 deals with a method for selection of events recorded by different Groza detectors that may be of interest for the study of processes in the thunderstorm atmosphere. The main results of experiments carried out in the season of 2007 are described at some length in Section 5. Worthy of special note are observations of short but intense gamma-ray bursts in the active phase of thunderstorms. Specific RB – EAS discharges caused by the combined action of RB and an EAS in the thunderstorm atmosphere were recorded for the first time. The discovery of long (10–100 ms) intense gamma-ray bursts and their correlation with radio emission gives the first experimental evidence of the key role of RB in charge accumulation and transfer from clouds to the lightning leader during the active thunderstorm period.

2. Notes on the theory of runaway breakdown

2.1 Asymptotic solution

The breakdown problem in a kinetic theory is formulated as follows. The kinetic equation for electrons in the coordinate space **r** and momentum space **p** is considered. In the simplest representation, electric field E, number density N of neutral molecules, their charge Z, and other structural parameters of matter determining electron–electron collisions are assumed to be constant. The collision integral for electrons is taken in the linear form. Then, the solution of the kinetic equation for the electron distribution function $f(\mathbf{p}, t)$ — homogeneous, independent of spatial coordinates, and asymptotic in time t — has an exponential character:

$$f(\mathbf{p}, t) \to f_{01}(p) \exp(\nu_1 t) + f_{02}(\mathbf{p}) \exp(\nu_2 t) .$$

Here, ν_i is the eigenvalue of the linear kinetic equation, $i = 1, 2$, and $f_{0i}(\mathbf{p})$ is the corresponding eigensolution.

The exponential growth of the distribution function, hence the number of electrons, is what is known as electric breakdown of matter. Parameter ν_i defines the ionization frequency, and $\nu_i^{-1} \approx \tau_i$ is the characteristic time of breakdown. The co-existence of two independent solutions of the linear kinetic equation suggests the presence of two types of breakdown, conventional (ν_1) and RB (ν_2), in any dielectric.

2.2 Similarity relations

Runaway breakdown occurs in all kinds of matter. Because fast electrons interact with other electrons according to the Coulomb law, the character of interaction is always the same; therefore, RB possesses an identical structure in all substances and remarkable similarity properties, meaning that the critical electric field E_c in any matter is proportional to its density ρ. If ρ is expressed in grams per cm^3, then one finds

$$E_c = 1.8\rho \ [\text{MeV cm}^{-1}] .$$

Accordingly, the critical runaway electron energy ε is related to the electric field strength E by the expression

$$\varepsilon \cong \frac{m_e c^2}{2\delta} ,$$

where $\delta = E/E_c$.

The characteristic breakdown length l determines the growth scale of the RB exponent:

$$l = \frac{6.1}{\rho\delta^2} \text{ [cm]} .$$

It can be seen that l rapidly falls with increasing electric field strength ($\sim \delta^{-2}$).

Characteristic breakdown time τ_2 also decreases ($\sim\delta^{-3/2}$), while ionization frequency grows:

$$\tau_2 \cong 10^{-10}\rho^{-1}\delta^{-3/2} \text{ [s]} ,$$
$$\nu_2 \cong 10^{10}\,\rho\delta^{3/2} \text{ [s}^{-1}\text{]} .$$

In dense matter with $\rho \approx 10-100$ g cm^{-3}, characteristic breakdown times are extremely small and rapidly decrease as parameter δ grows.

Notice that the above similarity relations hold in a limited region of parameter δ variations:

$$1.5 \leqslant \delta \leqslant 100-150 .$$

2.3 Runaway breakdown in the atmosphere

Figure 2 depicts RB ionization frequency ν_2 in the air depending on the electric field strength E. Evidently, the frequency monotonically increases with E ($\sim E^{3/2}$), whereas the ionization frequency ν_1 of ordinary breakdown first grows very rapidly with E (roughly as $\sim E^{5.5}$) and then becomes saturated [21–23].

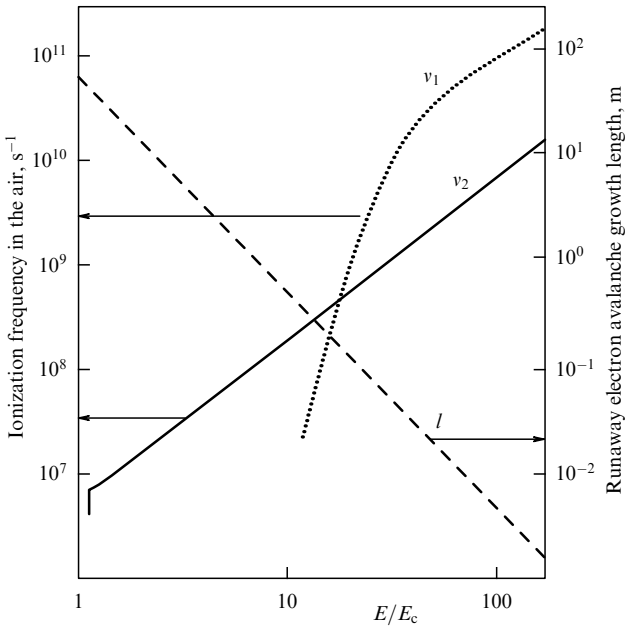

Figure 2. Dependences of ionization frequency in the case of conventional (ν_1) and runaway (ν_2) breakdown in the air on the electric field (left scale). Also shown is field dependence of runaway electron avalanche growth length (right scale).

Importantly, RB is possible even at low values of the electric field, i.e., in a *weak field*, provided the condition $E_{th} > E > E_c$ is met. In this case, the ionization frequency is rather high:

$$\nu_2 > 10^7 - 10^8 \text{ s}^{-1} .$$

Conventional electric breakdown in a weak field is impossible and occurs only if $E > E_{th}$. Despite rapid elevation of the ionization frequency of an ordinary breakdown with E, it remains lower than that of RB as the field grows up to $E \simeq 2E_{th}$. This fact is of great importance since it may lead to the appearance of a large number of fast electrons in a normal discharge for $2E_{th} \geqslant E \geqslant E_{th}$. It may be a cause of observed gamma-ray bursts both in a lightning leader [24–26] and in laboratory discharges [27–29].

Thus, RB proves to be the predominant breakdown in the air in terms of ionization rate, not only for $E < E_{th}$ but also at higher field strengths up to $E = 2E_{th}$.

The second important parameter plotted in Fig. 2 is characteristic length l that determines the minimal spatial scale of the breakdown region. It is seen that the characteristic length in weak fields $E \sim E_c$ is rather large ($l \approx 30-50$ m). However, it rapidly decreases ($\sim E^{-2}$) with increasing electric field strength to become 10–30 cm at $E \approx (1-2)E_{th}$. In high fields, $E \gg E_{th}$, the characteristic length l is quite small. This means that RB studies at low electric fields are feasible only in thunderstorm clouds, whereas at higher fields RB effects can just as well be observed in laboratory experiments.

2.4 The effect of cosmic rays

As noted above, fast bare electrons with an energy in excess of runaway energy ($\varepsilon > \varepsilon_c$) are needed for RB to occur, besides fulfillment of the condition $E > E_c$. The two conditions are satisfied in thunderstorm clouds. It has been found experimentally that maximally strong electric fields in the atmosphere thunderstorm clouds are close to the critical RB field E_c [1, 2, 9]. Secondary CR electrons having the relatively high mean flux density $\Phi_e \approx 10^3$ m^{-2} s^{-1} at altitudes of 4–8 km behave like fast bare particles in thunderstorm clouds.

An essential difference of RB from conventional electric breakdown consists in efficacious generation of X-ray and gamma radiation. It is the observation of gamma emission with an energy of $\varepsilon \sim 50-100$ keV that suggests the possibility of RB. Simultaneous excitation of strong electric currents promotes intense generation of radio emission.

Naturally, the number of runaway electrons is proportional to the number of bare ones resulting from the interaction between primary CRs in the atmosphere. The total number N_e of bare electrons in an EAS increases in proportion to the energy of a primary CR particle. By way of example, the shower formed by a primary particle with energy $E_{CR} \approx 10^{15}$ eV contains 10^6 bare electrons; at $E_{CR} \approx 10^{18}$ eV, $N_e \approx 10^{10}$.

The passage of an EAS through a thunderstorm cloud with $E > E_c$ gives rise to an avalanche of runaway electrons that cause an exponential rise in the number of high-energy electrons in the EASs. Simultaneously, the number of thermal electrons increases millions of times. Collectively, they produce an RB – EAS discharge [30]. Owing to the huge number of high-energy electrons, this discharge should be naturally accompanied by a strong pulse of gamma-ray radiation.

3. Groza experimental installation

The Groza installation comprises the following facilities: an EAS registering system, the system of NaI scintillation detectors, two independent radiosystems, a detector of jumps in the static electric field and its high-frequency component (Fig. 3). The maximum spacing between the detectors in the horizontal plane runs to 2–2.5 km, which enables observation of both temporal and spatial distributions of different forms of radiation in the clouds by intensity (and even monitoring movements of radiation sources together with the clouds). The relief of the Tien Shan station is very convenient for carrying out such surveys: the two closely spaced slopes near the mountain pass harboring the station allow the radiation detection sites to be located at different altitudes (from 3.4 to 4 km) above sea level. This makes it possible to obtain radiation distribution profiles inside the clouds, not only in the horizontal but also in the vertical plane.

3.1 Registering system of extensive air showers

The EAS registering system consists of a few dozen SI5G Geiger counter-based detectors spread over the area of the station to record the passage of an EAS, and to measure its size and primary particle energy. Each EAS detector contains 20 SI5G gas-discharge counters with parallel anodes; its sensitive area is around 0.6 m^2. Each detector occupies a specific location. Their mutual alignment is shown in Fig. 3. All EAS detectors are screened with 10-cm-thick iron filters to suppress the background of low-energy electrons. The adjacent detectors are spaced roughly 65 m apart. The sensitive area of the entire system is around 0.1 km^2.

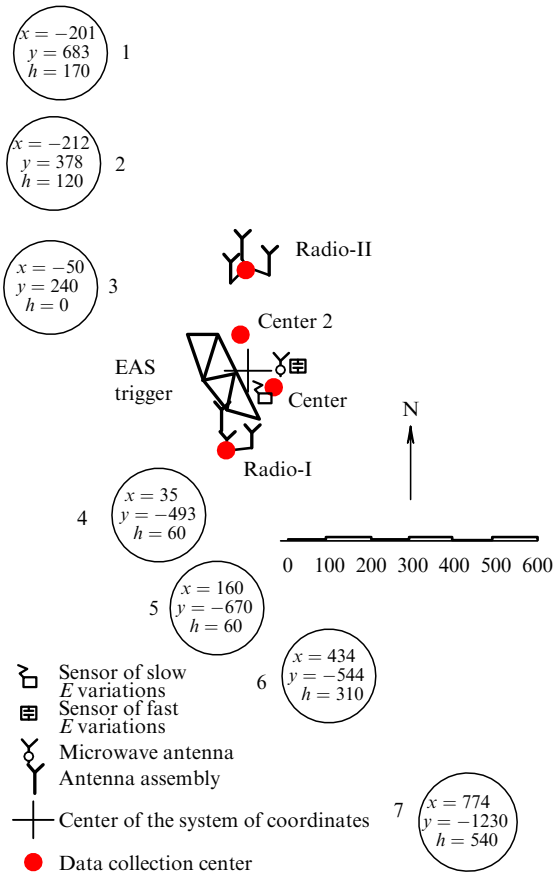

Figure 3. Groza experimental installation: polygon — EAS recording system (EAS trigger); circles (1–7) — array of NaI scintillation detectors, with numerals in the circles specifying coordinates (in meters) with respect to the Center (TSCRS) altitude; two independent radiosystems (Radio-I, Radio-II); detectors of 'fast' and 'slow' electric fields. Relative positions of all TSCRS facilities are to a scale.

3.2 System of gamma-ray scintillation detectors

Soft gamma radiation and hard X-ray radiation from electrons accelerated in the electric fields of a thunderstorm cloud are registered by 14 NaI crystal-based scintillation detectors. Seven registering sites are arrayed at the slopes of the surrounding mountains in a chain running across the usual direction of thunderstorm cloud movements (see Fig. 3). The distance between the ends of the chain reaches ≈ 2 km, and maximum vertical spacing between the detectors equals ≈ 600 m. Such a structure of the scintillation system makes it possible to study the spatial distribution of radiation inside thunderstorm clouds in both vertical and horizontal directions.

Two scintillation detectors are placed at each site. In one of them, an NaI crystal connected with an FEU-49 photoelectron multiplier is enclosed in an aluminium jacket with 1-mm-thick walls (Sc-II); in the other, the crystal is placed in a polyethylene tube with 10-mm-thick walls (Sc-I). As a result, the two detectors have different registering thresholds for gamma-ray radiation. In addition, one 'sham' FEU-49 detector without an NaI crystal is installed at several of the most remote sites from the system center (sites 1, 2, 6, and 7 in Fig. 3). The signals of these detectors serve to monitor electromagnetic pickup by the cables connecting the detectors with the observatory campus.

A particle passing through the NaI crystal of a scintillation detector produces electric pulses with a varying amplitude proportional to the energy dissipated by the charged particle or gamma quantum inside the crystal (for complete absorption in the crystal, the amplitude is proportional to the primary particle or quantum energy). Signals of the scintillators are transmitted to fast-acting amplitude analyzers (a set of parallelly-operating amplitude discriminators tuned to six startup thresholds). Output signals of the discriminators are pulses with the standard amplitude and duration, the intensity of which is estimated separately for each of the six amplitude ranges using a count-conversion algorithm. Absolute energy calibration of the detectors was performed with the use of ^{241}Am and ^{137}Cs gamma sources.

The intensity of gamma radiation emitted during the passage of thunderstorm clouds was measured in the high time-resolution mode. The intensity of signals from each scintillator was deduced from a time scan consisting of 4000 successive 200-μs intervals; this allows the time scan of short radiation bursts to be thoroughly analyzed. At each instant of continuous operation, the time scanning system stores the scintillation pulse intensity in memory for the past 0.8 s. If it receives a trigger signal during this time, the data collection system goes on working for another 0.4 s, after which the information is written to the disk of the master computer. In this way, the time sweep of signal intensity with a resolution of 200 μs 0.4 s before and after the arrival of each trigger signal is preserved for each recorded event.

3.3 Radiosystems

The electromagnetic radiation of thunderstorm discharges was studied with the employment of two radiosystems

(Radio-I and Radio-II in Fig. 3) operating in a frequency range of 0.1–30 MHz and recording the waveform of radiation pulses with a time resolution of around 16 ns. Also, the systems determined the direction to radiation sources from the relative time delays of radio signals [18, 19]. Each radiosystem has three antennas: two frame ones crossed at 90° to measure the horizontal magnetic component, and a whip antenna measuring vertical electric component of the electromagnetic field.

The radiosystems operate in the external trigger mode with a total recording duration of 200 ms and a prehistory (i.e., the record length before the arrival of the trigger pulse) of 160 ms.

The third Radio-E system is used to register ultrashort (metric) radiowaves at ~ 250 MHz. This system also contains detectors measuring electric field variations in the thunderstorm atmosphere: a quasistatic 'slow' field is measured with a 'field mill' electrostatic fluxometer, and electric field variations in the frequency range of 0.5–25 kHz ('fast' field) with a capacitor type sensor.

4. Selection of events for analysis

Indispensable for the study of CR and RB effects on the development of discharges in a thunderstorm atmosphere are continuous EAS monitoring; recording of short bursts of gamma-ray, X-ray, and radio emission, and elucidation of time correlations between them in time. The runaway breakdown theory implies that short gamma-ray and X-ray bursts from thunderstorm clouds have to result from an avalanche of high-energy electrons accelerated in the electric field of a thunderstorm cloud. Secondary CR electrons serve as bare electrons having the energy necessary for acceleration. Specifically, discharges initiated by the passage of EASs through the atmosphere may be ignited in thunderstorm clouds due to CR particles with energy $E_{CR} \geqslant 10^{15}$ eV. These physical mechanisms of burst generation were taken into account in the choice of conditions for generating trigger signals to be used in the registering system.

4.1 The trigger of extensive air showers

The shower trigger was implemented to study time correlations between the instant of EAS passage and gamma-ray, X-ray and radio emission. Its signal developed when pulses from four neighboring detectors of the shower-recording system coincided within the interval of 5 μs. Configuration of the shower trigger system illustrated in Fig. 3 permits one to effectively select an EAS with primary particle energy $E_{CR} \geqslant 10^{15}$ eV.

4.2 The trigger of an electric field jump

The trigger of an electric field jump was utilized to investigate intensity variations of gamma-ray, X-ray, and radio emission associated with the initiation and development of lightnings in a thunderstorm atmosphere. Because a cloud–earth discharge is accompanied by a rapid fall (for a few microseconds) in the electric field strength, the trigger signal was formed by a sensor of electric field variations at the instant of a sharp change ('jump') in the field strength. We chose a high startup threshold for the trigger-generating device, which corresponded to very closely spaced lightning discharges. This accounted for the small number of trigger signals of this type.

4.3 The electromagnetic trigger

Because the length of the cables connecting remote detectors with the data collection center amounted to 2 km, electromagnetic pulses produced by atmosphere discharges in the vicinity of the detector array were induced on long cables. Such a pulse coinciding with the in-cloud discharge was also used as the trigger signal.

4.4 Statistics of recorded events

The measurement data yielded by the Groza experiments were analyzed by comparing two samples of events: one obtained in clear cloudless weather, the other during the traversing of dense electrically charged clouds with lightning discharges over the TSCRS mountain pass. In the latter case, the uppermost detection sites (6 and 7 in Fig. 3) proved to be located deeper in the thunderstorm cloud than those at lower altitudes.

The total number of events recorded during both measurement periods is shown in Table 1.

Table 1. Statistics of events recorded in clear weather and during thunderstorms.

Type of event	Number of events in clear cloudless weather for 11 hours (13 August 2007)	Number of events during a thunderstorm for 11 hours (4, 7, 8, 15 August 2007)
EAS triggers	611	600
Number of events per hour	55 ± 2	54 ± 2
Events with EAS triggers containing short gamma-ray bursts	0	14
Triggers of an electric field jump	0	13
Electromagnetic triggers	0	503

It should be noted that an EAS trigger and a trigger of an electric field jump initiated both scintillation detectors and radiosystems. Electromagnetic triggers failed to develop under normal conditions but were formed by a discharge close to the cable. Therefore, statistics of relevant events fully reflect only those registered by scintillation detectors. Time synchronization of the readings of the scintillation detectors and radiosystems actuated by the electromagnetic trigger unambiguously suggest their correlation.

5. Results of the Groza experiments

5.1 Long-lasting gamma bursts and their correlation with radio emission

In most cases, strong electromagnetic pulses giving rise to an electromagnetic trigger result in powerful gamma-ray bursts. A typical example of gamma bursts registered upon initiation of scintillation detectors by the electromagnetic trigger is given in Fig. 4 showing the time-base sweep of signal intensity measured by one of the two scintillators (with a lower energy threshold for registering gamma quanta) located at sites 4, 6, and 7. The time scans for each detector are presented in three energy regions differing in lower amplitude thresholds corresponding to the minimal energy of recorded

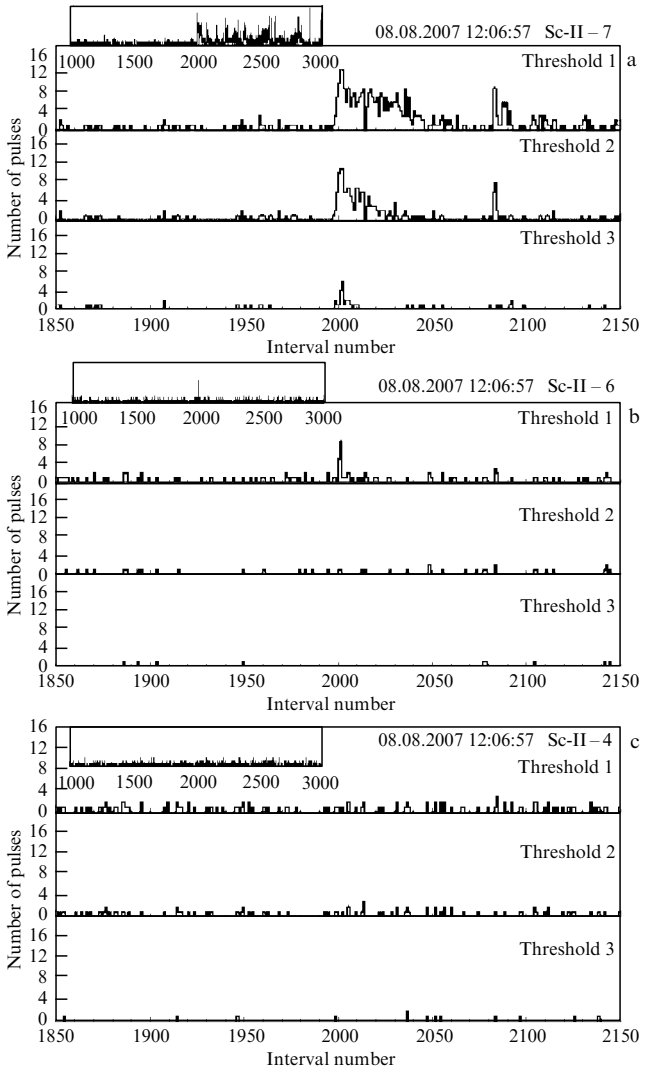

Figure 4. Gamma-ray bursts registered upon initiation of scintillation detectors by the electromagnetic trigger. The intensities are shown for three detection sites: (a) 7 (540 m above TSCRS), (b) 6 (310 m), and (c) 4 (TSCRS level). For each site, intensities of one counter are shown at three registering thresholds corresponding to the minimal energy of the recorded gamma quanta (30, 60, and 120 keV).

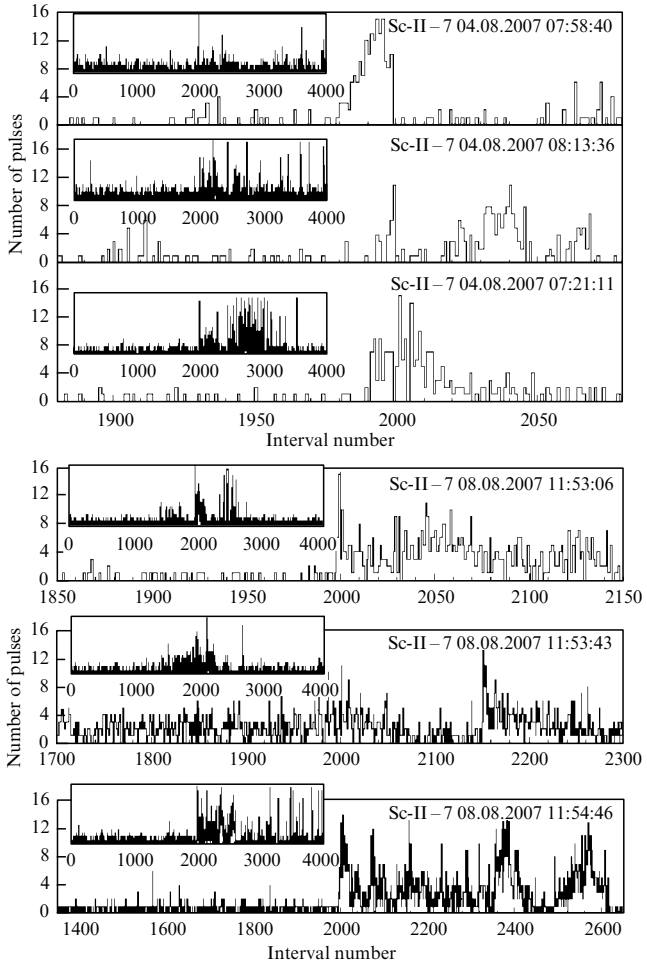

Figure 5. Time scans of gamma radiation intensity recorded with the electromagnetic trigger at 540 m above TSCRS (site 7) by the Sc-II detector with a threshold of 30 keV.

gamma quanta (30, 60, and 120 keV). The axes of abscissas in Fig. 4 are graduated in sequential numbers (200-microsecond time scan intervals); interval No. 2000 corresponds to the arrival of the trigger.

It appears from the top graph (4a) that the uppermost scintillation detector (site 7) begins to record enhanced gamma radiation 200–400 μs before the electromagnetic trigger. This radiation grows very rapidly, reaches a maximum when the trigger arrives, and persists for the next 10 ms. The inset to the top graph displays numerous similar flashes generated up to the 3000th time interval (200 ms after trigger actuation).

The background level of the signals throughout the first 1600 intervals of the time scan being considered amounts to 0.35 ± 0.01 pulses per interval. This value increases to 10–12 in the flash maximum, which corresponds to a rise in gamma radiation intensity by a factor of 30–35. Mean signal intensity during the first flash (from the 1998th to the 2046th interval) is 5.9 ± 0.3 pulses per interval (17 times above the background). Signal intensity throughout the flash duration rapidly decreases with gamma quanta energy, even if it remains an order of magnitude higher than the background value. Mean flash intensity in the second energy region (with a threshold of 60 keV) reaches 3.0 ± 0.3 pulses per interval (15 times the background value), and in the third one (120 keV) only 0.6 ± 0.1 pulses per interval (10 times the background value). In light of these statistics, the observed effect shows itself beyond any doubt.

Figure 4b illustrates the intensity of gamma quanta recorded (at three different energy thresholds) by a detector located 230 m below the previous one. The same flash is much weaker and manifests itself only in signals with a minimal energy threshold. Finally, the detector placed even lower (another 130 m down) (Fig. 4c) does not record any noticeable peculiarities at the instant of discharge.

The above character of radiation flashes is very typical and well apparent in most time scans of events registered by scintillation detectors inside thunderstorm clouds during electric discharges. Such flashes accompany at least 80% of the events recorded during a thunderstorm with a field jump trigger or an electromagnetic trigger; however, they do not occur in clear weather. This means that flashes are due to the presence of electrically charged clouds over detection sites. Examples of other events with long-lasting gamma bursts are presented in Fig. 5. Specifically, the uppermost graph in Fig. 5

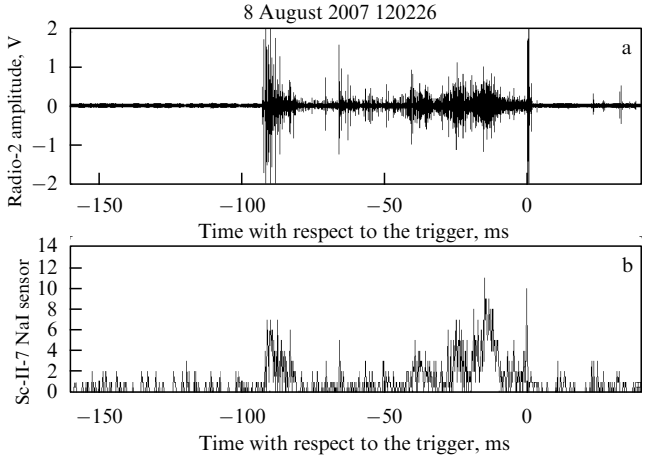

Figure 6. Radiofrequency radiation (a) and gamma-ray bursts (b) recorded with the use of an electromagnetic trigger.

shows a sharp cutoff of the gamma burst upon actuation of the electromagnetic trigger. Probably, it was the first return stroke of a lightning because radio emission died out for some time after it. Here (see the time scan), we observe similar attenuation of gamma activity.

A characteristic of long gamma-ray bursts is the distribution of their radiation in the vertical plane; all such bursts are especially well apparent at the uppermost detection site located deep in the thunderstorm cloud. The main signal component is built up by pulses with the lowest energy threshold. Thus, it can be concluded that the region where the bursts are generated lies in the depth of the thunderstorm cloud, while the bulk of radiation thus produced consists of low-energy gamma quanta.

In the above examples, the role of the trigger was played by a pulse of electromagnetic radiation created by an electric discharge. At the same instant of time, the scan displays a strong gamma pulse, suggesting close correlation between an electric discharge in the thunderstorm atmosphere and gamma-ray bursts. This is confirmed by the simultaneous observation of gamma and radiofrequency radiation. An example in Fig. 6 demonstrates close synchronization between gamma and radiofrequency radiation during a span of 100 ms.

5.2 Intercloud discharge induced by an extensive air shower (RB – EAS discharge)

An analysis of the time scans of the events presented in Table 1 permits distinguishing four short intense gamma-ray bursts in a thunderstorm atmosphere, which exactly coincide in time with the EAS trigger. One such an event occurred at the beginning of a thunderstorm on 15 August 2007, and the remaining three in the active phase of another thunderstorm (8 August 2007). Let us consider two of these events, one in the initial phase, the other in the active phase.

The first event (August 15, 2007) occurred during a thunderstorm that lasted 4 hours (from 05:18 to 09:40). The event occurred at 05:18:40 at the outset of the thunderstorm. EAS was recorded by all 6 detectors of the EAS trigger system. This means that the EAS was generated by a CR particle with an energy of 10^{16} eV or higher. The gamma pulse was registered at three sites (7, 6, and 4). The time scan of gamma-quantum intensity is presented in Fig. 7. The following characteristic features of this flash can be distinguished: (1) a strong gamma pulse was simultaneously detected at all detection sites; (2) the flash duration felt within a single time scan interval, i.e., was less than 200 μs; (3) the instant of gamma flash at all detection sites exactly coincided with the arrival of EAS, and (4) a sharp drop in background gamma radiation was recorded at the same instant of time.

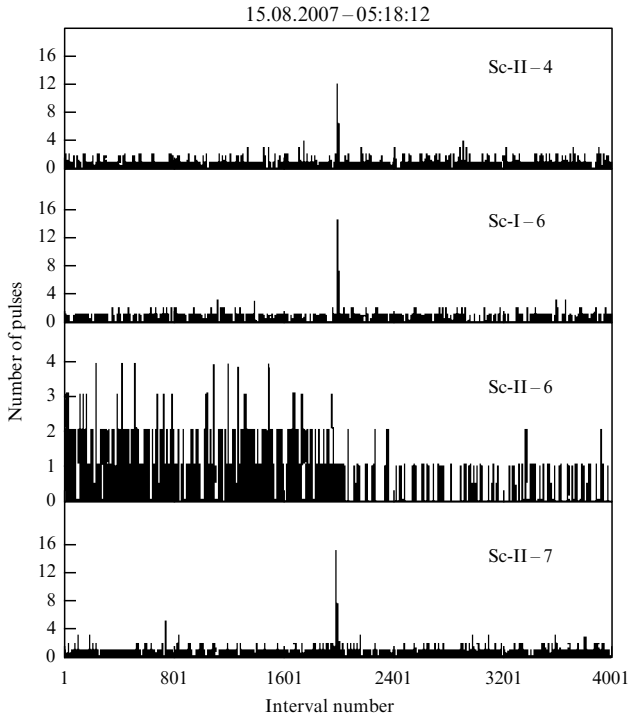

Figure 7. Time scan of gamma radiation intensity in an event exactly coincident in time with the EAS trigger. The event occurred at the beginning of a thunderstorm.

Notice that the distance between sites 4 and 7 is roughly 1100 m in the horizontal and 600 m in the vertical plane (see Fig. 3). In other words, strong gamma radiation extended over a large area. Also, Fig. 7 shows that the observed energy distribution of gamma quanta has the form of classical RB (see Section 5.3), i.e., a small difference between the cases of 30 keV (first threshold) and 60 keV (second threshold) and a sharp fall in the case of 120 keV (third threshold).

An abrupt change in the gamma-ray background at sites 6 and 7 (see Fig. 7) deserves special attention. The mean background value at site 6 decreases by a factor of 3 exactly at the moment of the trigger. At site 7, the background grows for 50 ms before the moment of the trigger and sharply decreases by approximately 3 times upon its arrival. The elevated gamma background created by CR is a consequence of enhancement of the fast electron flux in the strong thunderstorm field under the effect of RB[1]. The sharp decrease in the background reflects a sudden reduction in the electric field strength of the cloud crossed by EAS. In other words, an electric discharge in the cloud results from the

[1] Note a recent paper [33] where a long-term elevation of gamma background caused by fast electrons was observed during a thunderstorm at a height of 2770 m. The elevation lasted for 90 s, and the data were one-second averaged. The authors attributed the elevation to the enhancement of CR gamma background to RB effect. (*Authors' note to English translation.*)

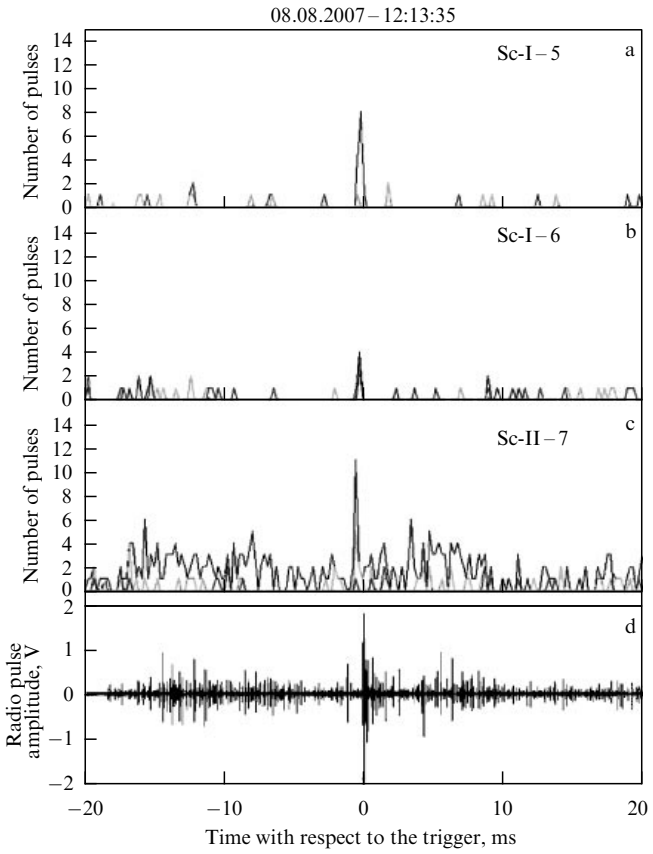

Figure 8. An event that occurred in the active phase of a thunderstorm, in which the instant of a gamma flash exactly coincided in time with that of the EAS trigger and radio emission: scans (a–c) show the time of the flash registered by scintillation detectors at sites 4, 6, and 7 with respect to the trigger pulse; scan (d) reveals the coincidence between radiofrequency and trigger pulses.

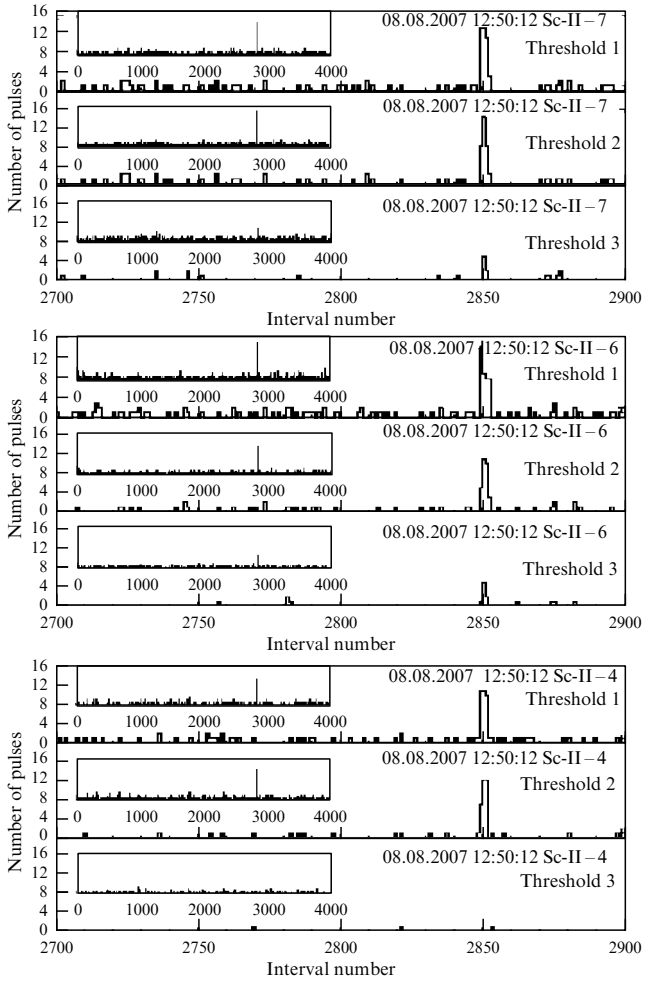

Figure 9. Time scans of gamma radiation intensity recorded by scintillation detectors using the EAS trigger. The scan sequence is similar to that in Fig. 4.

macroscopic effect of the joint RB/EAS action. Thus, we directly observe an RB–EAS discharge.

An event that took place in the active phase of the thunderstorm on 8 August 2007 is presented in Fig. 8. The thunderstorm lasted 1 hour (from 11:50 to 12:50). The event occurred at 12:35 during the active phase of the thunderstorm. An EAS was recorded at four detection sites. This means that the energy of the CR particle was at least 10^{15} eV. A strong gamma pulse was registered at sites 5, 6, and 7. The time scans of gamma radiation in Fig. 8 show that the strong gamma-ray pulse coincided with the EAS trigger at all detection sites. Figure 8d depicts in addition the measured radio signal. The strong pulse of radio emission is exactly coincident in time with the moment of EAS trigger, and gives evidence that the passage of the EAS through the thunderstorm cloud was accompanied by a strong electric discharge.

The above events give evidence of direct observation of RB–EAS discharges. This phenomenon was first examined in experiment. The probability of observation depends on two main factors. First, the path of a primary CR particle inducing the RB–EAS discharge must traverse a thunderstorm cloud at a distance of no more than 400–500 m from the gamma-ray scintillation detectors. Otherwise, the gamma emission will be absorbed in the atmosphere and remain undetected. On the other hand, the same path must be registered by the EAS-recording system. These conditions impose strong constraints on the number of permissible trajectories. Second, the strength E of the electric field in the cloud crossed by the EAS must be higher than the critical RB field: $E > E_c$. The latter condition is more frequently fulfilled in the active phase of a thunderstorm. The necessity to meet both conditions mentioned above reduces the probability of directly observing RB–EAS discharges to one in 100 'simple' EASs. We have observed only 4 RB–EAS discharges of the 600 recorded with the EAS trigger.

As noted above, the theory predicted the possibility of RB–EAS discharge, regarding it as one of the most important events in the thunderstorm atmosphere. Specifically, it associated the RB–EAS discharge with the high-altitude intercloud NBE discharge [8]. Characteristic features of NBE, namely, huge power of the radio pulse, weak optical radiation, absence of a step leader, and complete development within a few microseconds, agree with predictions of the RB–EAS discharge theory [31]. However, the RB–EAS discharge has never been directly observed.

5.3 Gamma spectrum of the lightning step leader

Analysis of all 600 events recorded with the EAS trigger showed that 14 included short intense gamma-ray flashes 400–800 μs in duration. Typical short gamma flashes registered by scintillation counters are presented in Figs 9 and 10 showing time scans of signal intensity from SC-II scintillators

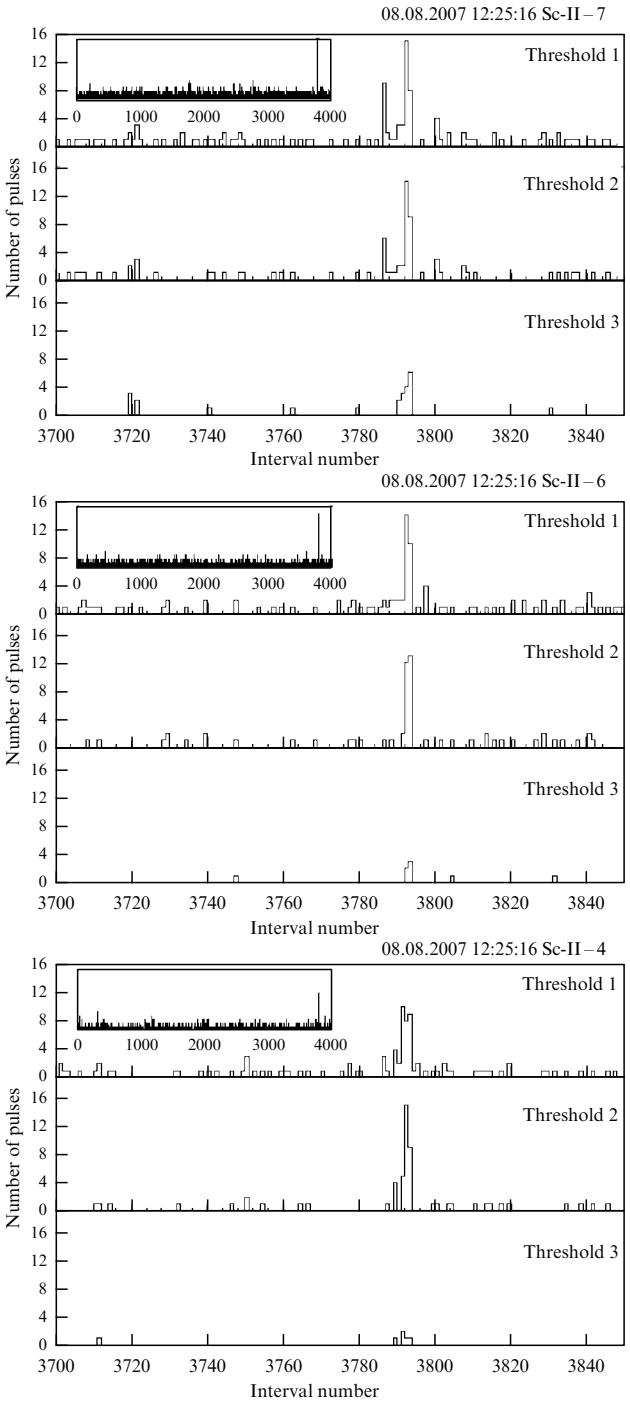

Figure 10. An event with a short gamma-ray flash similar to that in Fig. 9.

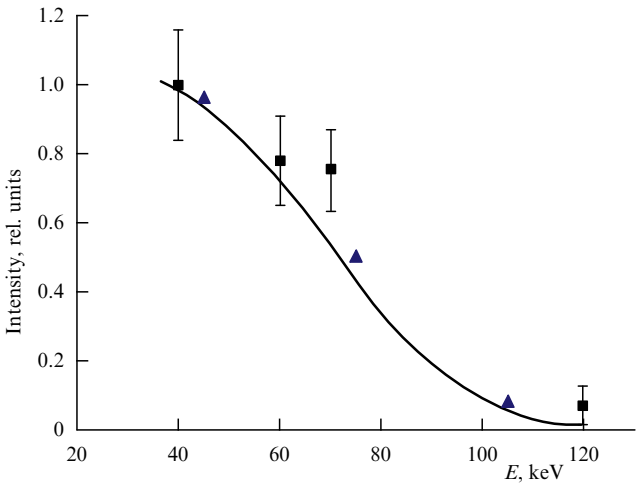

Figure 11. Integral spectrum of short gamma flashes recorded in thunderstorm events in the atmosphere: squares (with vertical error bars) — data of the Groza experiment; triangles — data of a balloon experiment, and solid line — theoretical curve.

(with a lower energy threshold for recording gamma-quanta energy) located at sites 4, 6, and 7. Figure 9 illustrates the event in which the intense gamma-ray burst occurred 170 ms after trigger actuation. The burst was 400–600 μs long and spread over a distance of around 1 km, since it was simultaneously seen at four detection sites (7, 6, 4, and 3) and at all energy thresholds. The time scan of another event is displayed in Fig. 10.

We analyzed 14 events to reconstruct the energy spectrum of gamma quanta. We counted the number of gamma quanta with energies above 30, 40, 60, 70, 120, and 320 keV in these events for each scintillation detector that recorded them, taking into account detector calibration results. The comparison of observations with different energy thresholds at all detection sites showed that their integral spectra look alike. The characteristic spectrum thus obtained is represented in Fig. 11. Mean gamma-quantum energy in a short flash was estimated at 80 keV.

Short gamma-ray bursts associated with the lightning step leader were reported in Ref. [24]. It was shown that they significantly correlate with step leader jumps [25]. Recent studies of this phenomenon have demonstrated that gamma radiation is generated in the step leader prior to the return stroke and lasts 200–400 μs [26], during which the leader covers a distance of 200–400 m. This distance is a measure of gamma-quanta absorption in the atmosphere at sea level. Absorption at the TSCRS altitudes is 1.5 times lower, being proportional to the air density. It is therefore natural to suggest that the short (400–800 μs) intense gamma-ray bursts observed in our experiments actually emanate from the step leader before the return stroke of a lightning. It may be assumed from the theory that gamma radiation in the case of RB is generated in the leader's typical electric field $E \simeq 2E_{\rm th}$ (see Section 2.3). Then, the RB ionization frequency should strongly depend on the macroscopic parameters of the medium, such as electric field strength E and molecular number density $N_{\rm m}$. At the same time, the energy spectra of both runaway electrons and the gamma radiation they generate have the same characteristic shape.

In Fig. 11, the normalized integral spectrum predicted by the theory is compared with our experimental data. Evidently, the two spectra agree fairly well. The figure also shows the results of a balloon experiment during a thunderstorm at an altitude of 4 km [32]. Numerous balloon experiments demonstrated that the electric field in the atmosphere is rather weak (max. 3–9 kV cm^{-1} [6, 7]), and RB is initiated by secondary EAS electrons passing through the cloud. As follows from Fig. 11, the gamma spectrum obtained in the balloon experiment is in excellent agreement with both the theory and our observations. We interpret the results of our experiments on the assumption that RB is caused by fast electrons produced during electric breakdown in the air in the strong electric field (50–60 kV cm^{-1}) of the step leader's head. Thus, the integral RB spectrum is very similar in both experiments and agrees with the theory (see Section 2.3) despite the significant difference between the electric field

strengths in the cloud (3–9 kV cm^{-1}) and in the step leader (50–60 kV cm^{-1}).

6. Conclusion

This report considers selected data from the RB theory and the results of experimental studies concerned with thunderstorm events in the atmosphere. They are discussed with special reference to the active role of RB in the development of thunderstorm discharges.

Runaway breakdown is a novel and exceptionally common phenomenon underlain by Coulomb interactions between fast electrons and matter. We considered two new important issues of the RB theory. One is related to the proposed similarity relation that implies a similar RB structure in all substances. The other is the identification of a formerly unexplored strong region in the RB electric field: $2E_{\rm th} \geqslant E \geqslant E_{\rm th}$. Both conventional and runaway electric breakdowns are feasible at such field strengths. However, the ionization frequency for RB, i.e., its growth rate, is higher than for usual breakdown. This means that RB may play an important role in this region. These features are characteristic of the leader in a spark discharge and, perhaps, in a lightning leader.

The main achievement of the reviewed studies is the discovery of intense gamma-ray bursts in a thunderstorm cloud during the active phase of the discharge. The difficulty is posed by the fact that thunderstorm discharges are random and rapidly developing large-scale phenomena, hence the importance of drawing an analogy to lengthy spark discharges investigated under laboratory conditions. One element of a spark discharge is the leader transporting the electric charge. There is a similar leader in a thunderstorm discharge. The fast and extremely powerful return stroke of the lightning has been thoroughly investigated. However, a distinctive feature of spark discharges is the presence of an electrode that shed the electric charge accumulated in the capacitor; in a thunderstorm cloud, the charge is carried by water droplets and small pieces of ice over a large area (km-scale). How is such a charge collected from these structures and delivered to the leader within a few milliseconds? This problem has not thus far been discussed at any length in the literature. Electrical conduction of the air is not high enough for charge transfer and needs to be increased by at least 5–6 orders of magnitude.[2] It is still lower in the clouds. The cloud electric field measured many times in experiment is insufficient for direct breakdown of the air. Therefore, mechanisms underlying accumulation and transport of the charge to the lightning leader remained enigmatic (see Refs [3, 4, 34]). The discovery of intense gamma radiation and its correlation with radio emission suggests that RB may play a key role in these processes.

Thunderstorm clouds contain electric fields stronger than the RB critical field. The number of secondary EAS electrons entering the area of 1 km^2 for 1 ms amounts to $\sim 10^6$. They serve as a 'seed' for RB. Further studies are needed to clarify whether they can ensure fulfillment of necessary conditions for the charge transfer from a cloud to the lightning leader.

The results of Groza experiment underway at FIAN's TSCRS gave an idea of the mechanism behind electric charge accumulation from thunderstorm clouds for initiation of the lightning. Another new fact discovered in this experiment is an RB – EAS-induced discharge. The theory predicts that this discharge may be a source of narrow bipolar events (NBEs).

To sum up, the development of the active phase of a thunderstorm discharge (from preliminary breakdown to initiation of the leader and its propagation until the occurrence of return stroke) is totally governed by the accumulation and transfer of the electric charge from the clouds. Our study demonstrated that this process is accompanied by correlated powerful gamma-ray and radio emission fluxes created by runaway breakdown.

It is safe to conclude that runaway breakdown initiated by cosmic rays is the main driving mechanism of thunderstorm discharge.

The authors thank V P Antonova, L I Vil'danova, K P Zybin, G G Mit'ko, A S Naumov, M O Ptitsyn, Yu V Shlyugaev for the enlightening discussions of issues touched upon in this report.

The work was supported by RFBR grant 09-02-00462-a and EOARD grant 067004 (ISTC 3641p).

[2] More correctly, "...3–4 orders of magnitude." (*Authors' note to English translation*.)

References

1. Marshall T C et al. *Geophys. Res. Lett.* **32** L03813 (2005)
2. Stolzenburg M et al. *Geophys. Res. Lett.* **34** L04804 (2007)
3. Bazelyan E M, Raizer Yu P *Fizika Molnii i Molniezashchity* (Physics of Lightning and Lightning Protection) (Moscow: Fizmatlit, 2001)
4. MacGorman D R, Rust W D *The Electrical Nature of Storms* (New York: Oxford Univ. Press, 1998)
5. Sentman D D et al. *Geophys. Res. Lett.* **22** 1205 (1995)
6. Pasko V P et al. *Nature* **416** 152 (2002)
7. Smith D M et al. *Science* **307** 1085 (2005)
8. Jacobson A R *J. Geophys. Res.* **108** (D2) 4778 (2003)
9. Marshall T C, McCarthy M, Rust W *J. Geophys. Res.* **100** (D4) 7097 (1995)
10. Rhodes C et al. *J. Geophys. Res.* **99** (D6) 13059 (1994)
11. Gurevich A V, Zybin K P *Usp. Fiz. Nauk* **171** 1177 (2001) [*Phys. Usp.* **44** 1119 (2001)]
12. Gurevich A V, Zybin K P *Phys. Today* **58** (5) 37 (2005)
13. Gurevich A V, Milikh G M, Roussel-Dupre R *Phys. Lett. A* **165** 463 (1992)
14. Bethe H *Ann. Physik* **5** 325 (1930)
15. Wilson C T R *Proc. Cambr. Philos. Soc.* **22** 34 (1924)
16. Chubenko A P et al. *Phys. Lett. A* **309** 90 (2003)
17. Gurevich A V et al. *Phys. Lett. A* **325** 389 (2004)
18. Gurevich A V, Duncan L M , Karashtin A N, Zybin K P *Phys. Lett. A* **312** 228 (2003)
19. Karashtin A N, Shlyugaev Yu V, Gurevich A V *Izv. Vyssh. Uchebn. Zaved. Ser. Radiofiz.* **48** 800 (2005) [*Radiophys. Quantum Electron.* **48** 711 (2005)]
20. Antonova V P et al. *Zh. Tekh. Fiz.* **77** (11) 109 (2007) [*Tech. Phys.* **52** 1496 (2007)]
21. Borisov N D, Gurevich A V, Milikh G M *Iskusstvennaya Ionizirovannaya Oblast' v Ionosfere* (Artificial Ionized Region in the Ionosphere) (Moscow: IZMIRAN, 1986)
22. Papadopoulos K et al. *J. Geophys. Res.* **98** (A10) 17593 (1993)
23. Gurevich A V, Borisov N D, Milikh G M *Physics of Microwave Discharges* (Amsterdam: Gordon and Breach, 1997)
24. Moore C et al. *Geophys. Res. Lett.* **28** 2141 (2001)
25. Dwyer J R et al. *Geophys. Res. Lett.* **32** L01803 (2005)
26. Howard J et al. *Geophys. Res. Lett.* **35** L13817 (2008)
27. Dwyer J R et al. *Geophys. Res. Lett.* **32** L20809 (2005)
28. Rahman M et al. *Geophys. Res. Lett.* **35** L06805 (2008)
29. Nguyen C V, van Deursen A P J, Ebert U *J. Phys. D* **41** 234012 (2008)
30. Gurevich A V, Zybin K P, Roussel-Dupre R A *Phys. Lett. A* **254** 79 (1999)
31. Gurevich A V, Zybin K P, Medvedev Yu V *Phys. Lett. A* **349** 331 (2006)
32. Eack K et al. *J. Geophys. Res.* **101** 29637 (1996)
33. Tsushia H et al. *Phys. Rev. Lett.* **102** 255003 (2009)
34. Rakov V A, Uman M A *Lightning. Physics and Effects* (Cambridge: Cambridge Univ. Press, 2003)